Reliable Phase Stability Analysis for Asymmetric Models

Gang Xu[1], William D. Haynes[2*] and Mark A. Stadtherr[2†]

[1] Invensys/SimSci-Esscor, 26561 Rancho Parkway South, Suite 100, Lake Forest, CA 92630 USA

[2] Department of Chemical and Biomolecular Engineering, University of Notre Dame, 182 Fitzpatrick Hall, Notre Dame, IN 46556 USA

(March 2005)
(revised, June 2005)

Keywords: Phase stability; Phase equilibrium; Interval analysis; Validated computing; Equation of state; NRTL.

[*] Current address: NFS Inc., 1205 Banner Hill Road, Erwin, TN 37650 USA
[†] Corresponding author – Tel.: 574-631-9318; Fax: 574-631-8836; E-mail: markst@nd.edu

Abstract

A deterministic technique for reliable phase stability analysis is described for the case in which asymmetric modeling (different models for vapor and liquid phases) is used. In comparison to the symmetric modeling case, the use of multiple thermodynamic models in the asymmetric case adds an additional layer of complexity to the phase stability problem. To deal with this additional complexity we formulate the phase stability problem in terms of a new type of tangent plane distance function, which uses a binary variable to account for the presence of different liquid and vapor phase models. To then solve the problem deterministically, we use an approach based on interval analysis, which provides a mathematical and computational guarantee that the phase stability problem is correctly solved, and that thus the global minimum in the total Gibbs energy is found in the phase equilibrium problem. The new methodology is tested using several examples, involving as many as eight components, with NRTL as the liquid phase model and a cubic equation of state as the vapor phase model. In two cases, published phase equilibrium computations were found to be incorrect (not stable).

1. Introduction

A key step in the computation of multiphase equilibrium is phase stability analysis. A reliable technique for phase stability analysis will assure both that the correct number of phases is found, and that the phase split computed corresponds to a global minimum in the total Gibbs energy. That is, phase stability analysis serves as a global optimality test in solving the global optimization problem that determines phase equilibrium at constant temperature and pressure. However, phase stability analysis is itself a global optimization problem that can be very difficult to solve reliably. A standard approach to the problem is the use of tangent plane analysis [1], in particular the method implemented by Michelsen [2]. However, a very large number of other methods have been proposed, involving a variety of equation solving and optimization techniques. Some methods use local optimization and/or equation solving methods, perhaps in connection with some multistart approach, or the use of homotopy-continuation. Stochastic global optimization methods (e.g., simulated annealing, genetic algorithms, etc.) have also been frequently proposed in this context. However, none of these techniques is actually guaranteed to produce the correct results. Thus, there has been significant interest in the development of *deterministic* techniques that *guarantee* the correct solution of the phase stability problem, as reviewed briefly below. These efforts have been focused primarily on the case of symmetric models (same thermodynamic model used for all phases). Work on deterministic stability analysis for the asymmetric case (different models used for different phases) has been limited to cases involving either an ideal gas vapor phase or a pure solid phase. We will consider here a deterministic method for the more general asymmetric case, focusing on the common situation in modeling vapor-liquid equilibrium in which nonidealities are represented in the vapor phase by an equation of state and in the liquid phase by an excess Gibbs energy model.

One approach for deterministic phase stability analysis, as demonstrated by McDonald and Floudas [3,4,5,6] for symmetric cases in which various excess Gibbs energy models were used, is the use of deterministic global optimization techniques, such as GOP [7,8] and branch-and-bound [9]. McDonald and Floudas [3,4,5,6] also considered the asymmetric case in which an excess Gibbs energy model was used for liquid phases and the vapor was an ideal gas. A more general branch-and-bound strategy, the α-

BB method, was applied by Harding and Floudas [10] to symmetric cases in which cubic equation of state models were used. The α-BB approach relies on the use of convex underestimating functions to obtain lower bounds on the objective function. However, whether or not these are valid bounds depends on the proper choice of a parameter (α). Methods exist [11], based on an interval representation of the Hessian matrix, that can be used to guarantee a proper value of α, and this approach was applied by Harding and Floudas [10].

An alternative deterministic procedure for phase stability analysis is the use of an interval-Newton approach [12]. This has been demonstrated for symmetric cases using excess Gibbs energy models by Stadtherr et al. [13], McKinnon et al. [14], and Tessier et al. [15], and for symmetric cases using cubic equations of state by Hua et al. [16,17,18]. Recently Xu et al. [19] also applied this approach to the symmetric case in which a statistical associating fluid theory (SAFT) model is used. The interval-Newton procedure provides a *mathematical guarantee* that the phase stability problem is correctly solved. Moreover, since it uses interval arithmetic throughout, and thus bounds rounding error, the interval-Newton method also provides a rigorous *computational guarantee* of global optimality [20]. The interval-Newton approach will be applied here to the asymmetric case in which both liquid and vapor phases are nonideal.

In comparison to the symmetric model case, the use of multiple thermodynamic models in the asymmetric case adds an additional layer of complexity to the phase stability problem. To deal with this additional complexity we will formulate the phase stability problem in terms of a new type of tangent plane distance function, which uses a binary variable to account for the presence of different liquid- and vapor-phase models. To then solve the problem deterministically, we will use an interval-Newton approach. The new methodology is tested using several examples with NRTL as the liquid-phase model and a cubic equation of state as the vapor-phase model. In two cases, published phase equilibrium computations were found to be incorrect (not stable). In should be noted that, as recently demonstrated by Burgos-Solórzano et al. [21], procedures for deterministic phase stability analysis, such as described here, can be used in connection with any algorithm or software package for computing phase equilibrium, to validate the computed results and to provide corrective feedback if needed.

2. Problem Formulation

The basis for tangent plane analysis for phase stability is the test formulated by Baker et al. [1]. Assume that the phase to be tested has a composition (mole fraction) vector $\mathbf{x}_0$ and that a constant temperature T and pressure P have been specified. Then consider the molar Gibbs energy vs. composition (mole fraction) surface $g(\mathbf{x})$ and a hyperplane tangent to $g(\mathbf{x})$ at $\mathbf{x} = \mathbf{x}_0$. If this tangent plane ever crosses (goes above) the Gibbs energy surface, then the system being tested is not stable (i.e., it is either unstable or metastable). This condition is often stated in terms of the tangent plane distance function $D(\mathbf{x})$ that gives the distance of the Gibbs energy surface above the tangent plane. This is given by

$$D(\mathbf{x}) = g(\mathbf{x}) - g_0 - \mathbf{s}_0^{\mathrm{T}}(\mathbf{x} - \mathbf{x}_0), \tag{1}$$

where $g_0 = g(\mathbf{x}_0)$ and $\mathbf{s}_0 = \nabla g(\mathbf{x}_0)$ are the Gibbs energy function and its gradient evaluated at the feed composition $\mathbf{x}_0$. If $D(\mathbf{x})$ is negative for any value of $\mathbf{x}$, then the phase being tested is not stable. To determine if D is ever negative, its minimum is sought. If a stationary point (local minimum) of D is found for which $D < 0$, then this indicates that the phase being tested is not stable. Actually, to show that a phase it not stable, it is sufficient to find any point $\mathbf{x}$ for which $D < 0$. However, stationary points with $D < 0$ are commonly sought since they are useful in providing initial composition estimates for a possible new equilibrium phase or phases. Proof that the phase being tested is stable is obtained if the *global* minimum of D is zero (corresponding to the tangent point at the feed composition $\mathbf{x}_0$). Obviously this procedure may fail if the global minimum of the tangent plane distance function is not found. For instance, if the optimization algorithm used returns a global minimum of zero, while the true global minimum is negative, the conclusion that the phase is stable will be incorrect.

The foregoing assumes that there is a single function $g(\mathbf{x})$ that represents all phases that may be present in the system (though $g(\mathbf{x})$ may be multivalued if an equation of state model is used and there are multiple compressibility roots). Unlike this symmetric model case, in the asymmetric model case there will be different $g(\mathbf{x})$ functions for different types of phases. We will consider here only the situation in which vapor and liquid phases are possible, and use $g^{\mathrm{V}}(\mathbf{x})$ to represent the Gibbs energy of a vapor phase and $g^{\mathrm{L}}(\mathbf{x})$ to represent the Gibbs energy of liquid phases. Xu et al. [22] and Scurto et al. [23] have

described an approach for deterministic phase stability analysis for the asymmetric case of solid-fluid equilibrium, in which one model is used for fluid phases, and another for pure solid phases.

In tangent plane analysis for phase stability, since the goal in testing a phase is to detect alternate states that have a lower Gibbs energy, the Gibbs energy surface that must be used is given by whichever of $g^{\mathrm{V}}(\mathbf{x})$ and $g^{\mathrm{L}}(\mathbf{x})$ is lowest. That is, in Eq. (1), $g(\mathbf{x}) = \min[g^{\mathrm{V}}(\mathbf{x}), g^{\mathrm{L}}(\mathbf{x})]$, and evaluations at $\mathbf{x}_0$ must be done on the lower of the Gibbs energy surfaces. Thus,

$$\begin{aligned} D(\mathbf{x}) &= \min[g^{\mathrm{V}}(\mathbf{x}), g^{\mathrm{L}}(\mathbf{x})] - g_0 - \mathbf{s}_0^{\mathrm{T}}(\mathbf{x}-\mathbf{x}_0) \\ &= \min\begin{cases} g^{\mathrm{V}}(\mathbf{x}) - g_0 - \mathbf{s}_0^{\mathrm{T}}(\mathbf{x}-\mathbf{x}_0) \\ g^{\mathrm{L}}(\mathbf{x}) - g_0 - \mathbf{s}_0^{\mathrm{T}}(\mathbf{x}-\mathbf{x}_0) \end{cases} \\ &= \min[D^{\mathrm{V}}(\mathbf{x}), D^{\mathrm{L}}(\mathbf{x})]. \end{aligned} \tag{2}$$

Note that the vapor and liquid tangent plane distance functions, $D^{\mathrm{V}}(\mathbf{x}) = g^{\mathrm{V}}(\mathbf{x}) - g_0 - \mathbf{s}_0^{\mathrm{T}}(\mathbf{x}-\mathbf{x}_0)$ and $D^{\mathrm{L}}(\mathbf{x}) = g^{\mathrm{L}}(\mathbf{x}) - g_0 - \mathbf{s}_0^{\mathrm{T}}(\mathbf{x}-\mathbf{x}_0)$, respectively, are both based on the same values of g_0 and $\mathbf{s}_0$, as determined from whichever Gibbs energy surface is lower at $\mathbf{x}_0$. The minimization problem that then must be solved is

$$\begin{aligned} &\min_{\mathbf{x}}\{\min[D^{\mathrm{V}}(\mathbf{x}), D^{\mathrm{L}}(\mathbf{x})]\} \\ &\text{s.t. } 1 - \sum_{i=1}^{n} x_i = 0. \end{aligned} \tag{3}$$

In order to avoid the difficulties associated with the nondifferentiable objective function, it is convenient to reformulate the problem. We define the "pseudo tangent plane distance" function $\tilde{D}(\mathbf{x}) = \theta D^{V}(\mathbf{x}) + (1-\theta)D^{L}(\mathbf{x})$, where $\theta \in \{0,1\}$ is a binary variable whose value will be determined as part of the optimization problem. Assuming that an equation of state model $f(Z,\mathbf{x}) = 0$ is used for the vapor phase, and treating the compressibility Z as an independent variable, the minimization problem that must be solved can now be expressed as

$$\begin{aligned} &\min_{\mathbf{x},Z,\theta}\{\theta D^{\mathrm{V}}(Z,\mathbf{x}) + (1-\theta)D^{L}(\mathbf{x})\} \\ &\text{s.t. } 1 - \sum_{i=1}^{n} x_i = 0 \\ &\quad f(Z,\mathbf{x}) = 0 \\ &\quad \theta \in \{0,1\}. \end{aligned} \tag{4}$$

Using Lagrangian analysis, this optimization problem can also be represented by the equivalent system of nonlinear equations

$$\begin{aligned} &\frac{\partial \tilde{D}}{\partial x_i} - \frac{\partial \tilde{D}}{\partial x_n} = 0, \quad i = 1, \ldots, n-1 \\ &1 - \sum_{i=1}^{n} x_i = 0 \\ &f(Z, \mathbf{x}) = 0 \\ &\theta(1-\theta) = 0. \end{aligned} \tag{5}$$

Note that the last equation is equivalent to $\theta \in \{0,1\}$. This is an (n+2) × (n+2) system of nonlinear equations that can be solved for the stationary points in the optimization problem. As noted above, it is common to solve the phase stability problem by seeking such stationary points, since they may be useful in providing initial composition estimates for a possible new equilibrium phase or phases. The introduction of the binary variable θ is a key feature of this problem formulation, as it provides the capability to combine any two different thermodynamic models that might be used in an asymmetric model of phase behavior. While θ appears as a continuous variable in Eq. (5), it will be treated explicitly as a binary variable when this system is solved, as explained below.

The (reduced) Gibbs energy functions are expressed here relative to the pure components as liquids at system temperature and pressure. For a liquid phase

$$g^{\mathrm{L}}(\mathbf{x}) = \sum_{i=1}^{n} x_i \ln x_i + g^{\mathrm{E}}(\mathbf{x}), \tag{6}$$

where $g^{\mathrm{E}}(\mathbf{x})$ is the excess Gibbs energy as given by some appropriate model. The model used here is NRTL,

$$g^{\mathrm{E}}(\mathbf{x}) = \sum_{i=1}^{n} x_i \frac{\sum_{j=1}^{n} x_j \tau_{ji} G_{ji}}{\sum_{k=1}^{n} x_k G_{ki}}, \tag{7}$$

where $G_{ij} = \exp(-\alpha_{ij}\tau_{ij})$ and $\tau_{ij} = \dfrac{A_{ij}}{RT}$. In the examples below, the parameters A_{ij} and α_{ij} are taken from various literature sources. Though we will use NRTL here, the computational methodology described can be applied in connection with any model for the excess Gibbs energy (e.g., UNIQUAC, Wilson, etc.). For a vapor phase,

$$g^{\mathrm{V}}(Z,\mathbf{x}) = \sum_{i=1}^{n} x_i \ln x_i + \sum_{i=1}^{n} x_i \ln \hat{\phi}_i(Z,\mathbf{x}) - \sum_{i=1}^{n} x_i \left[v_i^{\mathrm{L}} \left(P - P_i^{\mathrm{sat}} \right) + \ln \phi_i^{\mathrm{sat}} + \ln \frac{P_i^{\mathrm{sat}}}{P} \right], \tag{8}$$

where $\hat{\phi}_i(Z,\mathbf{x})$ is the fugacity coefficient of component *i* in the mixture at system *T* and *P*, v_i^{L} is the molar volume of pure *i* as a liquid at system *T* (assumed independent of pressure and evaluated at saturation), P_i^{sat} is the vapor pressure of pure *i* at system *T*, and ϕ_i^{sat} is the fugacity coefficient of pure *i* as a vapor at P_i^{sat} and system *T*. The mixture fugacity coefficients $\hat{\phi}_i(Z,\mathbf{x})$ are determined here from a cubic equation of state model of the form

$$f(Z,\mathbf{x}) = Z^3 + b(\mathbf{x})Z^2 + c(\mathbf{x})Z + d(\mathbf{x}) = 0. \tag{9}$$

In the examples below, either the Peng-Robinson (PR) or Soave-Redlich-Kwong (SRK) equation of state is used, with standard van der Waals mixing rules. An equation of state can also be used to determine ϕ_i^{sat}; however, since P_i^{sat} is likely to be relatively small, it is often reasonable to assume that $\phi_i^{\mathrm{sat}} = 1$, and that is what is done here. Sources of data for the vapor-phase model parameters are discussed in the examples below.

3. Problem Solving Methodology

For solving Eq. (5), an (*n*+2) × (*n*+2) nonlinear system, for the stationary points in the phase stability problem, we use a method based on interval mathematics, in particular an interval-Newton approach combined with generalized bisection (IN/GB). This is a *deterministic* technique that provides a mathematical and computational *guarantee* that all the stationary points are found, and thus that the *global* minimum in the pseudo tangent plane distance function $\tilde{D}$ is found. For general background on interval mathematics, including interval arithmetic, computations with intervals, and interval-Newton methods, there are several good sources [20,24,25]. Details of the basic IN/GB algorithm employed here are given by Schnepper and Stadtherr [12] and Hua et al. [18].

An important feature of this approach is that, unlike standard methods for nonlinear equation solving and/or optimization that require a *point* initialization, the IN/GB methodology requires only an initial *interval*, and this interval can be sufficiently large to enclose all feasible results. Thus, in the case of phase stability analysis, all composition variables (mole fractions) x_i can be initialized to the interval

[0, 1]. For the vapor-phase compressibility factor Z an initial interval of [0.5, 1] is used. The lower limit of 0.5 effectively eliminates any liquid-like compressibility roots (the equation of state is used to represent the vapor phase only) and in most circumstances is reasonable for the relatively low pressures at which asymmetric models are typically used. If the pressure was so high that the vapor-phase compressibility was less than 0.5, then a symmetric model using an equation of state for both vapor and liquid phases would likely be used. Of course, the initial interval for Z can easily be modified as desired to fit other circumstances, as discussed further in Section 4.4 below. Finally, for the binary variable θ, the initial interval is set to [0, 1].

Intervals are searched for stationary points using powerful root inclusion tests based on the interval-Newton method. This method can determine with mathematical certainty if an interval contains no stationary point or if it contains a *unique* stationary point. In the algorithm used here, we first apply interval-Newton using the pivoting preconditioner described by Gau and Stadtherr [26]. If necessary, this is followed by a root inclusion test using the standard inverse-point preconditioner [12]. If, after both of the interval-Newton tests, it cannot be proven that that interval contains a unique stationary point or no stationary point, then the interval is bisected and the root inclusion tests applied eventually to each subinterval. For the binary variable θ, a special bisection rule is used. If θ is chosen by the IN/GB algorithm as the variable to be bisected, then it is bisected into the degenerate (thin) intervals [0, 0] and [1, 1]. Note that thus θ can be bisected only once. In this way, θ is treated explicitly as a binary (rather than continuous) variable in solving the equation system.

On completion, the IN/GB algorithm will have determined narrow enclosures of *all* the stationary points of D, including the local and global optima, and thus the global minimum can be readily determined. Alternatively, IN/GB can be applied in connection with a branch-and-bound scheme, which will lead directly to the global minimum without finding any of the other stationary points. However, as noted above, if the tested phase is not stable, knowledge of the stationary points can be useful for initializing phase split computations.

4. Results and Discussion

Using this problem solving methodology, together with the concept of pseudo tangent plane distance, as introduced above, we now consider several test problems. In each case, an asymmetric model is used, with NRTL for the liquid phase, and a cubic equation of state (PR or SRK) for the vapor phase. The first two example problems are very simple and serve to demonstrate the key concepts of the methodology.

4.1 Problem 1

This problem involves the binary mixture of tetrahydrofuran (component 1) and 2,2,4-trimethylpentane (component 2). Du et al. [27] performed vapor-liquid equilibrium measurements for this system at P = 101.3 kPa, and then modeled their results using NRTL and SRK. They determined NRTL parameters by fit to experimental data, obtaining A_{12} = –225.523 cal/mol and A_{21} = 555.498 cal/mol, with $\alpha_{12} = \alpha_{21}$ fixed at 0.2. For SRK, they used the pure component properties (critical temperature, critical pressure and acentric factor) T_{c1} = 540.15 K, P_{c1} = 5188 kPa, ω_1 = 0.2264, T_{c2} = 543.96 K, P_{c2} = 2568 kPa, and ω_2 = 0.3031. The binary interaction parameter was taken to be k_{12} = 0. For this example, we will focus on phase stability at T = 350 K. At this temperature, from the physical property models used by Du et al., the vapor pressure values are $P_1^{sat} = 142.39$ kPa and $P_2^{sat} = 51.29$ kPa, and the saturated liquid molar volumes are $v_1^L = 87.89$ cm^3/mol and $v_2^L = 176.1$ cm^3/mol.

For this model, the Gibbs energy surface g for a phase of composition x_1 (and $x_2 = 1 - x_1$) is shown in Figure 1. Note that this surface is determined from the vapor-phase model g^V and liquid-phase model g^L using $g = \min[g^V, g^L]$. For an overall (feed) composition of $x_{0,1}$ = 0.6, the pseudo tangent plane distance (PTPD) function $\tilde{D}$ is shown in Figure 2. This shows that there are two stationary points in the PTPD, one at x_1 = 0.6 and $\theta = 1$ (the feed point; vapor phase) and the other at $x_1 \approx 0.33$ and $\theta = 0$. Because $\tilde{D}$ is negative at this latter point, this system is clearly not stable as a single phase. Since $\theta = 0$ at the point where $\tilde{D}$ is negative, this indicates that the total Gibbs energy can be lowered by introducing a liquid phase.

The interval-Newton methodology outlined above was applied to compute the stationary points for several feed compositions for this system, with the results as shown in Table 1. The values reported

here (and in the subsequent tables) for the stationary points are point approximations of very narrow intervals that have been proven to contain a unique solution to Eq. (5). The feed composition of $x_{0,1} = 0.3$ is shown to be stable as a liquid ($\theta = 0$) and $x_{0,1} = 0.9$ is shown to be stable as a vapor ($\theta = 1$), since for these cases the global minimum of the PTPD is zero (at the feed point). The feed compositions of $x_{0,1} = 0.5$, $x_{0,1} = 0.6$, and $x_{0,1} = 0.65$ are shown to be not stable since they exhibit negative values for the PTPD. These results are consistent with the phase diagram computed by Du et al. [27] using the model described above. For each feed point considered, the computation time required to compute all the stationary points was approximately 0.01 s. These times, and all computation times reported below, were determined using an Intel Pentium 4 CPU (3.2 GHz).

4.2 Problem 2

For this problem we consider the binary mixture of dimethyl carbonate (component 1) and cyclohexane (component 2) at $T = 298.15$ K, the phase behavior of which was measured and modeled by Cocero et al. [28]. NRTL parameters were determined from experimental data as $A_{12} = 875.972$ cal/mol and $A_{21} = 937.397$ cal/mol, with $\alpha_{12} = \alpha_{21} = 0.47$. Vapor-phase nonidealities were modeled using PR, with pure component properties $T_{c1} = 539.0$ K, $P_{c1} = 4630$ kPa, $\omega_1 = 0.462$, $T_{c2} = 553.4$ K, $P_{c2} = 4070$ kPa, and $\omega_2 = 0.212$, and binary interaction parameter $k_{12} = 0$. At the system temperature of 298.15 K, the vapor pressure values used by Cocero et al. are $P_1^{\text{sat}} = 7.190$ kPa and $P_2^{\text{sat}} = 13.014$ kPa. Liquid molar volumes were taken to be $v_1^{\text{L}} = 84.693$ cm^3/mol and $v_2^{\text{L}} = 108.747$ cm^3/mol.

The interval-Newton methodology was applied to compute the stationary points for several feed compositions for this system at P = 16.5 kPa (close to a homogeneous azeotrope at about 16.8 kPa), with the results as shown in Table 2. Feeds at $x_{0,1} = 0.125$, $x_{0,1} = 0.325$, and $x_{0,1} = 0.75$ are shown to be stable as single-phase liquid, vapor, and liquid, respectively, since in each case the global minimum of the PTPD is zero. For the feeds at $x_{0,1} = 0.275$ and $x_{0,1} = 0.45$, negative values of the PTPD are observed, so these are not stable as a single phase. These results are all in agreement with the work of Cocero et al. [28]. For each feed point considered, the computation time required to compute all the stationary points was again approximately 0.01 s.

4.3 Problem 3

In this example, the system studied is the binary mixture of 2,3-dimethyl-2-butene (component 1) and methanol (component 2). Experimental vapor-liquid equilibrium measurements were made for this system recently by Uusi-Kyyny et al. [29] at atmospheric pressure. The experimental pressure varied slightly, but for most measurements was P = 101.2 kPa, and this is the value used here. The experimental results were modeled by Uusi-Kyyny et al. using SRK as the vapor-phase model, and using NRTL, Wilson, and UNIQUAC as different liquid-phase models. Parameters in each of the liquid-phase models were estimated by minimizing the sum of the absolute values of the relative errors between the measured activity coefficient and the activity coefficient calculated from the model. To then test the liquid-phase models, Uusi-Kyyny et al. used them to perform bubble-point calculations at each of the liquid-phase compositions x_1 on the experimental vapor-liquid envelope. Comparing the computed results for the vapor-phase compositions y_1 and temperature T to the experimental values showed that the average errors were $\Delta y_1 = 0.0059$ and $\Delta T = 0.14$ K for the Wilson equation, $\Delta y_1 = 0.0124$ and $\Delta T = 0.41$ K for NRTL, and $\Delta y_1 = 0.0194$ and $\Delta T = 0.56$ K for UNIQUAC. So the Wilson equation apparently provided the best fit, followed by NRTL, and then UNIQUAC.

We will use the NRTL model here, with the parameters A_{12}/R = 691.87 K and A_{21}/R = 513.14 K ($\alpha_{12} = \alpha_{21} = 0.4$), as determined by Uusi-Kyyny et al. For SRK, the pure component properties used are T_{c1} = 524.0 K, P_{c1} = 3160 kPa, ω_1 = 0.2333, T_{c2} = 512.6 K, P_{c2} = 8096 kPa, and ω_2 = 0.5656, and the binary interaction parameter used is $k_{12} = 0$. Pure component vapor pressures come from the Antoine equation (with P_i^{sat} in MPa and T in K),

$$P_i^{\text{sat}} = \exp\left(A_i - \frac{B_i}{T + C_i} \right), \tag{10}$$

with A_1 = 6.574, B_1 = 2500.8, C_1 = –64.19, A_2 = 9.5334, B_2 = 3550.3 and C_2 = –37.353. The liquid molar volumes used are $v_1^{\text{L}} = 119.643$ cm^3/mol and $v_2^{\text{L}} = 40.7$ cm^3/mol. All the model parameters used here are exactly as given by Uusi-Kyyny et al.

As a test problem for the phase stability analysis procedure described above, we first chose a feed composition on the experimental vapor-liquid envelope, namely $x_{0,1}$ = 0.6233 and T = 325.62 K. Our

expectation was that this feed would either be just slightly outside the phase envelope predicted by NRTL/SRK, in which case the feed would test as stable, or it would be just slightly inside the phase envelope, in which case the feed would test as unstable, with one stationary point near the experimental vapor-phase composition (y_1 = 0.4758) showing a negative value of PTPD. However, what we actually computed for this feed composition was quite different, as shown in the first row of results in Table 3. This feed tested as not stable, but in addition to a stationary point with negative PTPD near the experimental vapor-phase composition, there were also two other stationary points with negative PTPD. Using NRTL/SRK to do a bubble-point calculation for this liquid-phase composition (x_1 = 0.6233) shows that there is a solution to the bubble-point problem at y_1 = 0.4684 and T = 325.243 K. This is very near the experimental values of 0.4758 (Δy_1 = 0.0074) and 325.62 K (ΔT = 0.377 K), and so presumably this is the solution obtained by Uusi-Kyyny et al. Now testing this result for phase stability, with the results shown in the second row of data in Table 3, as well as in the PTPD plot in Figure 3, shows that this solution to the bubble point problem is in fact not stable. While this may be a mathematically correct solution to the bubble point problem, it is not thermodynamically correct, and it is not a point on the vapor-liquid envelope predicted by NRTL/SRK, as was believed by Uusi-Kyyny et al. In fact, a phase split calculation, followed by phase stability analysis of the results (third row of results in Table 3), shows that for a feed of $x_{0,1}$ = 0.6233 at T = 325.243 K, NRTL/SRK predicts *liquid-liquid* equilibrium, with one liquid phase of composition x_1 = 0.29703 and another liquid phase with composition x_1 = 0.85822.

In Figure 4, we show the entire phase diagram for this system when calculated from Uusi-Kyyny et al.'s SRK/NRTL model, along with the experimental phase equilibrium data. These calculations were validated by using the methodology for phase stability analysis described above. Stability analysis results are given for some selected points in Table 3 (for each feed tested in this table the computation time was less than 0.05 s). Clearly the phase diagram calculated from the model does *not* closely match the experimental data. Experimentally, a *homogeneous* azeotrope is observed; however, the model predicts a *heterogeneous* azeotrope (VLLE line). The model predicts that there should be no liquid phases observed with compositions in the range from roughly x_1 = 0.298 to x_1 = 0.858 (end points on the VLLE line), but in fact there are many experimental liquid-phase points seen within this range. These discrepancies

between model and experiment are plainly due to the fact that Uusi-Kyyny et al.'s model predicts a liquid-liquid split, while experimentally this apparently does not occur. The prediction of a liquid-liquid split is due solely to the liquid-phase model used, and so it is clear that the NRTL parameters given by Uusi-Kyyny et al. are not correct. Uusi-Kyyny et al. [29] were misled into thinking their NRTL parameters were reasonable values because the phase stability procedure they used (if any) was apparently not reliable, and thus they did not recognize that their model predicted a liquid-liquid split. This does not necessarily mean that NRTL is a poor choice of model for the liquid, only that a poor choice of parameters has been made.

4.4 Problem 4

This example is based on the work of Kang [30], who did measurements and modeling of vapor-liquid equilibrium for the system dichlorodifluoromethane (CFC-12) (component 1) and hydrogen fluoride (component 2) at T = 303.15 K. Measurements of equilibrium pressure and average liquid phase composition show that this system exhibits a maximum-pressure heterogeneous azeotrope, and a model is presented which appears to provide a good prediction of the pressure and the liquid-liquid phase split at the azeotrope. Kang's model uses NRTL for the liquid phase. For the vapor phase, the base model is Peng-Robinson, but there is an additional contribution to the equation of state to account for the association of HF molecules, as described by Łenko and Anderko [31]. For the computations done here, we will use the same liquid-phase model (NRTL) as Kang, but for the vapor phase, we will use the base PR model only, without the association terms. Thus we would expect our calculations to match liquid-liquid phase split results computed by Kang, but not to match Kang's results for vapor-phase compositions or equilibrium pressures.

For the NRTL model, the parameters obtained by Kang are A_{12} = 1595.631 cal/mol and A_{21} = 1701.751 cal/mol, with $\alpha_{12} = \alpha_{21} = 0.425$. For PR, the pure component properties used are T_{c1} = 385.0 K, P_{c1} = 4129 kPa, ω_1 = 0.179, T_{c2} = 461.0 K, P_{c2} = 6480 kPa, and ω_2 = 0.372, and the binary interaction parameter used is k_{12} = 0. At the system temperature of 303.15 K, the pure component vapor pressure values used by Kang are $P_1^{sat} = 742.73$ kPa and $P_2^{sat} = 144.0$ kPa. Liquid molar volumes were taken to

be $v_1^L = 95.804$ cm^3/mol and $v_2^L = 14.9$ cm^3/mol, from the modified Rackett equation with parameters given by Kang.

Kang computes a maximum-pressure heterogeneous azeotrope (VLLE line) at about 868 kPa, with the liquid splitting into one liquid phase with composition $x_1 \approx 0.06$ and other liquid phase with composition $x_1 \approx 0.90$ (values estimated from a plot). Since the liquid-phase model (NRTL) is pressure-independent, the same liquid-liquid split should be observed for pressures above the maximum-pressure heterogeneous azeotrope, where there should be liquid-liquid equilibrium only (no vapor). As an initial test point for our phase stability analysis procedure, we chose a pressure (905 kPa) somewhat above the heterogeneous azeotrope, and a composition ($x_{0,1} = 0.54$) in the middle of the presumed two-phase (liquid-liquid) region. Results of applying phase stability analysis for this point are shown in the first row of data in Table 4. This shows that actually this point is a *stable liquid* (single phase), and *not* in a two-phase region as Kang's computations would indicate. Further analysis shows that there is in fact a solution to the liquid-liquid equilibrium conditions (equal activity conditions) with $x_1 = 0.0652$ for the first liquid phase and $x_1 = 0.8993$ for the second liquid phase. This is clearly the phase split found by Kang for the heterogeneous azeotrope. Phase stability analysis shows, however, that this is not a stable liquid-liquid phase split, as indicated in Table 4 (second row) and in the PTPD plot in Figure 5. In fact, when Kang's model is correctly solved, by use of the reliable phase stability analysis procedure given here, there are two VLLE lines (one a heterogeneous azeotrope) found. At the heterogeneous azeotrope (slightly lower in pressure than Kang's incorrect azeotrope) and pressures above it, the liquid splits into one liquid phase with $x_1 = 0.5566$ and another liquid phase with $x_1 = 0.9013$. At the other VLLE line (slightly lower in pressure than the heterogeneous azeotrope) and pressures above it, the liquid splits into one liquid phase with $x_1 = 0.0647$ and another liquid phase with $x_1 = 0.5360$. Both these phase splits were validated using phase stability analysis, as indicated in Table 4 (third and fourth lines) for trial points (905 kPa) somewhat above the VLLE pressures. Since this type of phase behavior is not observed experimentally, and the prediction of a liquid-liquid split is due solely to the liquid-phase model used, it is apparent that the NRTL parameters determined by Kang are not appropriate. In a situation similar to that seen in the previous example, apparently the phase stability procedure used by Kang (if any) was not reliable, leading

to an incorrect liquid-liquid phase split result, and misleading Kang into thinking that his NRTL parameters were reasonable.

Figures 6 and 7 show a phase diagram computed for the pressure range near the three-phase lines. These calculations were validated by doing phase stability analysis using the methodology described above. Stability analysis results are given for some selected points in Table 4 (for each feed tested in this table the computation time was less than 0.1 s). It should be re-emphasized that the vapor-phase model used for these computations is not the same vapor-phase model used by Kang, and thus pressure and vapor-phase composition results are not directly comparable to Kang's results. In fact, since Kang's liquid-phase model is poor, as determined above, and our vapor-phase model is poor since it does not account for the association of HF, the phase diagram in Figures 6 and 7 is perhaps best regarded as that of a "hypothetical" system described by the NRTL/PR model given above.

Another issue that should be discussed in connection with this problem is the initial interval chosen for the vapor-phase compressibility Z. As discussed above, we generally specify a lower bound of 0.5 for Z. For standard cubic equations-of-state, such as PR and SRK, at the low pressures for which NRTL or other activity coefficient models are likely to be used, this is a very safe assumption. However, for a strongly associating fluid, such as HF, standard cubic equations of state are inadequate, and the vapor-phase compressibility could easily be below 0.5 even at conditions for which Z is close to one for most other compounds [31]. Since, in our "hypothetical" model, PR is used without vapor-phase association, we were still able to use a lower bound of 0.5. However, if the Łenko and Anderko model [31], which does account for vapor-phase association, was used, we would have needed to use a smaller lower bound for Z. We anticipate that, in most such cases, the modeler will be able to set the lower bound on Z based on physical knowledge of the system being modeled. If this is not possible, then the lower bound on Z can simply be set to the lowest feasible value consistent with the EOS being used. If this is done, however, stationary points from the EOS model ($\theta = 1$) might be found that have a liquid-phase, not vapor-phase, compressibility. Since the EOS is intended to model the vapor phase only, these stationary points would need to be screened out. This can be done by solving the EOS for the vapor-phase

compressibility at the composition of the stationary point, and then eliminating that stationary point if it does not correspond to the vapor phase.

4.5 Problem 5

This problem involves the ternary mixture of methyl acetate (component 1), methanol (component 2) and water (component 3) at P = 101.3 kPa, the phase behavior of which was measured and modeled by Martin and Mato [32]. For the liquid phase, the model used is NRTL-m, a variation of NRTL due to Mato et al. [33] in which α_{ij} is not an independent parameter but is instead determined from

$$\alpha_{ij} = \frac{1}{2 + G_{ij} G_{ji}}, \tag{11}$$

with G_{ij} as defined above. NRTL-m parameters were determined by fit to experimental data to be A_{12}/R = 168.9 K, A_{21}/R = 177.6 K, A_{13}/R = 521.3 K, A_{31}/R = 667.6 K, A_{23}/R = 333.2 K and A_{32}/R = –121.7 K. For the vapor phase, the model used is PR, with pure component properties T_{c1} = 506.85 K, P_{c1} = 4691 kPa, ω_1 = 0.327, T_{c2} = 512.58 K, P_{c2} = 8096 kPa, ω_2 = 0.569, T_{c3} = 647.35 K, P_{c3} = 22119 kPa, ω_3 = 0.348, and all binary interaction parameters set to zero. The liquid molar volumes used are $v_1^{\mathrm{L}} = 79.914$ cm^3/mol, $v_2^{\mathrm{L}} = 40.732$ cm^3/mol, and $v_3^{\mathrm{L}} = 18.07$ cm^3/mol. Pure component vapor pressures come from the Antoine equation (with P_i^{sat} in kPa and T in K), with A_1 = 14.2533, B_1 = 2665.54, C_1 = –53.424, A_2 = 15.8733, B_2 = 3242.87, C_2 = –49.550, A_3 = 16.5699, B_3 = 3984.92, and C_3 = –39.724, as given by Martin and Mato (whose expression for the Antoine equation contains a typographical error).

The interval-Newton methodology was applied to compute the stationary points for several feed compositions for this system, with the results as shown in Table 5. Each feed point tested is one on the experimental vapor-liquid envelope, and thus we would expect it to be either just outside or just inside the phase envelope predicted by the model. If the feed is just inside the predicted phase envelope, it should test as not stable, with a stationary point having a negative PTPD near the composition of the phase on the other side of the experimental tie line; or, if the feed is just outside the predicted phase envelope, then it should test as stable. For each feed point tested, this expectation is met. For example, an experimental tie line at T = 329.05 K connects a liquid phase of composition (0.472, 0.323, 0.205) and a vapor phase of composition (0.663, 0.263, 0.074). Using the liquid phase as the feed point, as shown in the first row of

data in Table 5, the stability test indicates that it is not stable, and there is a stationary point with a negative PTPD at (0.6543, 0.2719, 0.0739) and $\theta = 1$ (vapor), very near the experimental vapor phase composition. For each feed tested, the computation time was less than 0.2 s.

4.6 Problem 6

In this problem, we consider the five-component mixture of *n*-propanol (component 1), *n*-butanol (component 2), benzene (component 3), ethanol (component 4) and water (component 5). For the liquid phase, NRTL is used with the parameters as given by Tessier et al. [15]. For the vapor phase, PR is used with the pure component properties (T_c, P_c and ω) given in Table 6. Since we are primarily interested in this system as a test of computational performance, and not in the accuracy of the model, all binary interaction parameters k_{ij} are assumed to be zero. The values of the binary interaction parameters do not affect the mathematical form of the equation system to be solved, only the coefficient values, and thus by assuming all $k_{ij} = 0$, the problem is not necessarily made any more or less difficult. Table 6 also provides, for each component, the liquid molar volumes used, as well as constants for the Antoine equation (with P_i^{sat} in mmHg and T in K).

We used the interval-Newton methodology to determine stationary points for several feed mixtures for this system. Table 7 gives selected results, at different T and P, for feeds with composition (0.148, 0.052, 0.52, 0.10, 0.18). The first row of data, for T = 298.15 K and P = 101.325 kPa, corresponds to conditions used in one of the test problems given by Tessier et al. [15], who correctly assumed that there would be no vapor phase at these conditions. The liquid-phase stationary point results correspond directly to those given by Tessier et al. Computation time requirements are also given in Table 7, and range from 7.3 to 29.9 s, depending primarily on the number of stationary points that exist.

4.7 Problem 7

This final example is intended primarily to investigate the computational performance of the interval-Newton methodology as problem size (number of components) continues to increase. Hypothetical mixtures of up to eight components are used. The NRTL A_{ij} and α_{ij} parameters for these mixtures are given in Table 8. For the vapor phase, PR is used with the critical properties, acentric factor,

liquid molar volumes, and Antoine equation coefficients (for P_i^{sat} in mmHg and T in K) given in Table 6 for components 1–5, and in Table 9 for components 6–8 (note that though the pure component data used for components 1–5 are the same as used in Problem 6, the NRTL parameters used for components 1–5 are not the same as in Problem 6). The six component mixture studied involves components 1–6 and has a feed composition of (0.148, 0.052, 0.400, 0.100, 0.180, 0.120). The seven component mixture comprises components 1–7 with a feed composition of (0.148, 0.052, 0.300, 0.100, 0.180, 0.120, 0.100). The eight component mixture consists of components 1–8 and has a feed composition of (0.148, 0.052, 0.300, 0.100, 0.180, 0.120, 0.060, 0.040).

Table 10 gives results at selected temperatures and pressures for the three feeds and problem sizes considered. These results are representative of the range of computation time requirements encountered in solving these problems for several other temperatures and pressures. For each problem size, computation times range over roughly an order of magnitude, with higher computation time not necessarily corresponding to a larger number of stationary points. These results also reflect the exponential complexity that may be associated with deterministic global optimization (in general, an NP-hard problem). While multi-hour computation times, such as seen in the next to last problem in Table 10 for the eight component problem, may seem large, at least in this context, this time can be well spent if it means avoiding the computation of a phase equilibrium with the wrong number of phases.

5. Concluding Remarks

We have addressed here the problem of determining phase stability, in a reliable and deterministic way, for the case in which asymmetric modeling (different models for vapor and liquid phases) is used. To do this, we introduced a new type of tangent plane distance function, which uses a binary variable to account for the presence of different liquid and vapor phase models. To then solve the problem deterministically, we used an interval-Newton approach, which provides a mathematical and computational guarantee that the global minimum, as well as all the stationary points, in the tangent plane distance function are found. The new methodology was successfully tested using several examples, involving as many as eight components, with NRTL as the liquid phase model and a cubic equation of

state as the vapor phase model. In two cases, published phase equilibrium computations were found to be incorrect (not stable).

The guarantee that the phase stability problem is correctly solved clearly comes at the expense of additional computation time, which may become large as problem sizes become large. Thus, this procedure is not well suited for situations in which it would be used repeatedly inside some other iterative calculation, such a process simulator, or a stand-alone code for phase equilibrium. Instead, the most appropriate use for this procedure is as a *final validation* step, to determine whether the process simulator, or stand-alone phase equilibrium code, has in fact reached a correct result. The use of deterministic phase stability analysis in this context has recently been demonstrated by Burgos-Solórzano et al. [21], who also show how the stationary point results can be used to provide corrective feedback in the case that a phase equilibrium result is determined to be incorrect. Because of the additional computational expense, a modeler may ultimately need to consider the trade-off between the computation time expense and the risk of getting the wrong answer to the phase equilibrium problem of interest. As the example problems considered demonstrate, this risk is not insignificant. The additional computation time used to validate a result may be especially well spent in "mission critical" situations, in which errors in the number or composition of equilibrium phases present is not tolerable.

Acknowledgement

This work has been supported in part by the donors of The Petroleum Research Fund, administered by the ACS, under Grant 35979-AC9, by the National Science Foundation Grant EEC97-00537-CRCD, by the Environmental Protection Agency Grant R826-734-01-0. and by The State of Indiana 21st Century Fund under Grant #031500-0077.

List of Symbols

A_i Antoine equation coefficient

A_{ij} NRTL parameter

B_i Antoine equation coefficient

C_i Antoine equation coefficient

D tangent plane distance

$\tilde{D}$ pseudo tangent plane distance

g molar Gibbs energy

G_{ij} NRTL parameter

k_{ij} binary interaction parameter

n number of components

P pressure

R gas constant

T temperature

v molar volume

$\mathbf{s}$ gradient of g

$\mathbf{x}$ composition (mole fraction) vector

Z compressibility

Greek letters

α_{ij} NRTL parameter

θ binary variable used to define pseudo tangent plane distance

τ_{ij} NRTL parameter

ϕ fugacity coefficient

$\hat{\phi}$ mixture fugacity coefficient

ω acentric factor

Subscript

c indicates critical property

0 indicates evaluation at feed composition

Superscripts

E indicates an excess property

L indicates quantity for the liquid phase

sat indicates evaluation at saturation

V indicates quantity for the vapor phase

References

[1] L. E. Baker, A. C. Pierce, K. D. Luks, Soc. Petrol, Eng. J. 22 (1982) 732-742.

[2] M. L. Michelsen, Fluid Phase Equilib. 9 (1982), 1-19.

[3] C. M. McDonald, C. A. Floudas, AIChE J. 41 (1995) 1798-1814.

[4] C. M. McDonald, C. A. Floudas, Comput. Chem. Eng. 19 (1995) 1111-1139.

[5] C. M. McDonald, C. A. Floudas, Ind. Eng. Chem. Res. 34 (1995) 1674-1687.

[6] C. M. McDonald, C. A. Floudas, Comput. Chem. Eng. 21 (1997) 1-23.

[7] C. A. Floudas, V. Visweswaran, Comput. Chem. Eng. 14 (1990) 1397-1417.

[8] C. A. Floudas, V. Visweswaran, J. Optim. Theory Appl. 78 (1993) 187-225.

[9] J. E. Falk, R. M. Soland, Manag. Sci. 15 (1969) 550-569.

[10] S. T. Harding, C. A. Floudas, AIChE J. 46 (2000) 1422-1440.

[11] C. S. Adjiman, S. Dallwig, C. A. Floudas, A. Neumaier, Comput. Chem. Eng. 22 (1998) 1137-1158.

[12] C. A. Schnepper, M. A. Stadtherr, Comput. Chem. Eng. 20 (1996) 187-199.

[13] M. A. Stadtherr, C. A. Schnepper, J. F. Brennecke, AIChE Symp. Ser. 91(304) (1995) 356-359.

[14] K. I. M. McKinnon, C. G. Millar, M. Mongeau, in State of the Art in Global Optimization: Computational Methods and Applications (C. A. Floudas, P. Pardalos, Eds.), Kluwer Academic Publishers, Dordrecht, The Netherlands (1996), pp. 365-382.

[15] S. R. Tessier, J. F. Brennecke, M. A. Stadtherr, Chem. Eng. Sci. 55 (2000) 1785-1796.

[16] Z. Hua, J. F. Brennecke, M. A. Stadtherr, Fluid Phase Equilib. 116 (1996) 52-59.

[17] J. Z. Hua, J. F. Brennecke, M. A. Stadtherr, Comput. Chem. Eng. 20 (1996) S395-S400.

[18] J. Z. Hua, J. F. Brennecke, M. A. Stadtherr, Ind. Eng. Chem. Res. 37 (1998) 1519-1527.

[19] G. Xu, J. F. Brennecke, M. A. Stadtherr, Ind. Eng. Chem. Res. 41 (2002) 938-952.

[20] E. Hansen, G. W. Walster, Global Optimization Using Interval Analysis, Marcel Dekker, New York, 2004.

[21] G. I. Burgos-Solórzano, J. F. Brennecke, M. A. Stadtherr, Fluid Phase Equilib. 219 (2004) 245-255.

[22] G. Xu, A. M. Scurto, M. Castier, J. F. Brennecke, M. A. Stadtherr, Ind. Eng. Chem. Res. 39 (2000) 1624-1636.

[23] A. M. Scurto, G. Xu, J. F. Brennecke, M. A. Stadtherr, Ind. Eng. Chem. Res. 42 (2003) 6464-6475.

[24] R. B. Kearfott, Rigorous Global Search: Continuous Problems, Kluwer Academic Publishers, Dordrecht, The Netherlands (1996).

[25] A. Neumaier, Interval Methods for Systems of Equations, Cambridge University Press, Cambridge, UK (1990).

[26] C.-Y. Gau, M. A. Stadtherr, Comput. Chem. Eng. 26 (2002) 827-840.

[27] T.-B. Du, M. Tang, Y.-P Chen, Fluid Phase Equilib. 192 (2001) 71-83.

[28] M. J. Cocero, F. Mato, I. García, J. C. Cobos, H. V. Kehiaian, J. Chem. Eng. Data 34 (1989) 73-76.

[29] P. Uusi-Kyyny, J.-P. Pokki, Y. Kim, J. Aittamaa, J. Chem. Eng. Data 49 (2004) 251-255.

[30] Y. W. Kang, J. Chem. Eng. Data 43 (1998) 12-16.

[31] M. Łenko, A. Anderko, AIChE J. 39 (1993) 533-538.

[32] M. Martin, R. B. Mato, J. Chem. Eng. Data 40 (1995) 326-327.

[33] F. A. Mato, R. B. Mato, F. Mato, Ind. Eng. Chem. Res. 28 (1989) 1441-1446.

Table 1. Results for selected feed compositions in Problem 1.

Feed ($x_{0,1}, x_{0,2}$)	Stationary Points[a] (x_1, x_2); θ; Z	PTPD ($\widetilde{D}$)	Result
(0.3, 0.7)	(0.3, 0.7); 0 (0.5696, 0.4304); 1; 0.9641	0 0.1224	Stable (L)
(0.5, 0.5)	(0.5, 0.5); 0 (0.7229, 0.2771); 1; 0.9684	0 –0.04808	Not Stable
(0.6, 0.4)	(0.6, 0.4); 1; 0.9650 (0.3336, 0.6664); 0	0 –0.08891	Not Stable
(0.65, 0.35)	(0.65, 0.35); 1; 0.9664 (0.3953, 0.6047); 0	0 –0.03328	Not Stable
(0.9, 0.1)	(0.9, 0.1); 1; 0.9729 (0.8110, 0.1890); 0	0 0.2358	Stable (V)

[a] A value of the compressibility Z is given only for vapor-phase stationary points ($\theta = 1$).

Table 2. Results for selected feed compositions in Problem 2.

Feed ($x_{0,1}, x_{0,2}$)	Stationary Points[a] (x_1, x_2); θ; Z	PTPD ($\widetilde{D}$)	Result
(0.125, 0.875)	(0.125, 0.875); 0 (0.2680, 0. 0.7320); 1; 0.9917	0 0.0102	Stable (L)
(0.275, 0.725)	(0.275, 0.725); 1; 0.9917 (0.1351, 0.8649); 0	0 –0.005216	Not Stable
(0.325, 0.675)	(0.325, 0.675); 1; 0.9917 (0.2789, 0.7211); 0	0 0.02073	Stable (V)
(0.45, 0.55)	(0.45, 0.55); 0 (0.3474, 0.6526); 1; 0.9917	0 –0.01873	Not Stable
(0.75, 0.25)	(0.75, 0.25); 0 (0.3927, 0.6073); 1; 0.9917	0 0.03095	Stable (L)

[a] A value of the compressibility Z is given only for vapor-phase stationary points ($\theta = 1$).

Table 3. Results for selected feed compositions and temperatures in Problem 3.

Feed ($x_{0,1}, x_{0,2}$) T (K)	Stationary Points[a] (x_1, x_2); θ; Z	PTPD ($\widetilde{D}$)	Result
(0.6233,0.3767) 325.62	(0.6233,0.3767); 0 (0.4678,0.5322); 1; 0.9693 (0.2923,0.7077); 0 (0.8551,0.1449); 0	0 –0.01439 –0.006359 –0.004804	Not Stable
(0.6233,0.3767) 325.243	(0.6233,0.3767); 0 (0.4684,0.5316); 1; 0.9692 (0.2914,0.7086); 0 (0.8559,0.1441); 0	0 0 –0.006428 –0.004878	Not Stable
(0.85822,0.14178) 325.243	(0.85822,0.14178); 0 (0.29703,0.70297); 0 (0.4691,0.5309); 1; 0.9692 (0.6125,0.3875); 0	0 0 0.005939 0.005537	Stable (LL)
(0.47,0.53) 325.5	(0.47,0.53); 1; 0.9692 (0.3093,0.6907); 0 (0.5913,0.4087); 0 (0.8618,0.1382); 0	0 0.004763 0.008723 0.001917	Stable (V)
(0.46,0.54) 325.5	(0.46,0.54); 1; 0.9695 (0.2448,0.7552); 0 (0.7603,0.2397); 0 (0.7954,0.2046); 0	0 –0.002933 0.01694 0.01692	Not Stable
(0.48,0.52) 325.5	(0.48,0.52); 1; 0.9689 (0.8845,0.1155); 0	0 –0.01404	Not Stable

[a] A value of the compressibility Z is given only for vapor-phase stationary points ($\theta = 1$).

Table 4. Results for selected feed compositions and pressures in Problem 4.

Feed ($x_{0,1}, x_{0,2}$) P (kPa)	Stationary Points[a] (x_1, x_2); θ; Z	PTPD ($\widetilde{D}$)	Result
(0.54, 0.46) 905.0	(0.54, 0.46); 0 (0.8151, 0.1849); 1; 0.8024 (0.2247, 0.7753); 0 (0.0649,0.9351); 0 (0.7796,0.2204); 0 (0.8985 ,0.1015); 0	0 0.001293 0.00604 0.0003998 0.002569 0.001201	Stable (L)
(0.0652055, 0.9347945) 905.0	(0.0652, 0.9348); 0 (0.8993, 0.1007); 0 (0.8152, 0.1848); 1; 0.8024 (0.2228, 0.7772); 0 (0.5446, 0.4554); 0) (0.7762, 0.2238); 0	0 0 0.0001724 0.005488 –0.0008581 0.001485	Not Stable
(0.5566258, 0.4433742) 905.0	(0.5566, 0.4434); 0 (0.9013, 0.0987); 0 (0.8156, 0.1844); 1; 0.8024 (0.2181, 0.7819); 0 (0.0659, 0.9341); 0 (0.7672, 0.2328); 0	0 0 0.0003807 0.007156 0.002048 0.0018	Stable (LL)
(0.0646917, 0.9353083) 905.0	(0.0647, 0.9353); 0 (0.5360, 0.4640); 0 (0.8150, 0.1850); 1; 0.8024 (0.2264, 0.7736); 0 (0.7826, 0.2174); 0 (0.8978, 0.1022); 0	0 0 0.001527 0.005776 0.002775 0.001505	Stable (LL)
(0.816, 0.184) 904.0	(0.816, 0.184); 1; 0.8027 (0.2133, 0.7867); 0 (0.0667, 0.9333); 0 (0.5700, 0.4300); 0 (0.7569, 0.2431); 0 (0.9033, 0.0967); 0	0 0.009177 0.004454 0.001125 0.002413 0.0002516	Stable (V)
(0.8, 0.2) 904.0	(0.8, 0.2); 1; 0.8021 (0.0470, 0.9530); 0	0 –0.07318	Not Stable

[a] A value of the compressibility Z is given only for vapor-phase stationary points ($\theta = 1$).

Table 5. Results for selected feed compositions and temperatures in Problem 5.

Feed ($x_{0,1}, x_{0,2}, x_{0,3}$) T (K)	Stationary Points[a,b] (x_1, x_2, x_3); θ; Z	PTPD ($\widetilde{D}$)	Result
(0.472, 0.323, 0.205) 329.05	(0.472, 0.323, 0.205); 0 (0.6543, 0.2719, 0.0739); 1; 0.9746	0 –0.01236	Not Stable
(0.101, 0.827, 0.072) 333.65	(0.101, 0.827, 0.072); 0 (0.2601, 0.7144, 0.0255); 1; 0.9789	0 0.001998	Stable (L)
(0.788, 0.075, 0.137) 331.05	(0.788, 0.075, 0.137); 1; 0.9743 (0.4547, 0.0846, 0.4606); 0	0 0.03545	Stable (V)
(0.152, 0.433, 0.415) 334.65	(0.152, 0.433, 0.415); 0 (0.4983, 0.3946, 0.1071); 1; 0.9776	0 –0.04126	Not Stable
(0.762, 0.136, 0.102) 328.25	(0.762, 0.136, 0.102); 0 (0.7750, 0.1546, 0.0704); 1; 0.9731	0 –0.005388	Not Stable

[a] Mole fractions may not sum precisely to one, due to rounding of computer output during transcription to the table.
[b] A value of the compressibility Z is given only for vapor-phase stationary points ($\theta = 1$).

Table 6. Pure component physical property data used in Problem 6. Antoine equation coefficients are for the case of P_i^{sat} in mmHg and T in K.

	$i = 1$	$i = 2$	$i = 3$	$i = 4$	$i = 5$
T_{ci} (K)	536.9	562.0	562.6	516.25	647.0
P_{ci} (kPa)	5200.0	4500.0	4924.39	6383.47	22064.0
ω_i	0.5687	0.125	0.209	0.636	0.225
v_i^L (cm^3/mol)	75.14	91.97	89.41	58.68	18.07
A_i	8.37895	7.36366	6.87987	8.11220	8.07131
B_i	1788.020	1305.198	1196.760	1592.864	1730.630
C_i	227.438	173.427	219.161	226.184	233.426

Table 7. Results for selected feeds in Problem 6. The feed composition in each case is (0.148, 0.052, 0.520, 0.100, 0.180).

Feed T (K) P (kPa)	Stationary Points[a,b] $(x_1, x_2, x_3, x_4, x_5)$; θ; Z	PTPD ($\widetilde{D}$)	CPU time[c] (s)	Result
298.15 101.325	(0.148, 0.052, 0.520, 0.100, 0.180); 0 (0.0343, 0.0010, 0.6810, 0.0979, 0.1857); 1; 0.9625 (0.1625, 0.0532, 0.2706, 0.1284, 0.3854); 0 (0.1633, 0.0564, 0.3969, 0.1161, 0.2674); 0 (0.0260, 0.0006, 0.0019, 0.0383, 0.9332); 0 (0.0796, 0.0263, 0.7840, 0.0577, 0.0524); 0	0 1.744 0.00008219 –0.0001011 –0.08658 –0.001902	29.9	Not Stable
348.15 101.325	(0.148, 0.052, 0.520, 0.100, 0.180); 1; 0.9751 (0.3353, 0.2881, 0.2273, 0.0528, 0.0964); 0	0 –0.2155	7.3	Not Stable
355.15 101.325	(0.148, 0.052, 0.520, 0.100, 0.180); 1; 0.9764 (0.3221, 0.2757, 0.2584, 0.0529, 0.0910); 0	0 0.07189	7.5	Stable (V)
388.15 500	(0.148, 0.052, 0.520, 0.100, 0.180); 0 (0.0859, 0.0067, 0.4516, 0.1297, 0.3261); 1; 0.9182 (0.1647, 0.0548, 0.3722, 0.1169, 0.2914); 0 (0.0502, 0.0030, 0.0081, 0.0542, 0.8845); 0	0 –0.03616 0.000503 –0.07101	13.6	Not Stable
418.15 900	(0.148, 0.052, 0.520, 0.100, 0.180); 1; 0.8526 (01655, 0.1490, 0.6037, 0.0436, 0.0383); 0	0 –0.06271	11.6	Not Stable

[a] Mole fractions may not sum precisely to one, due to rounding of computer output during transcription to the table.
[b] A value of the compressibility Z is given only for vapor-phase stationary points ($\theta = 1$).
[c] Intel Pentium 4 CPU (3.2 GHz)

Table 8. NRTL parameters A_{ij} (cal/mol) (top) and α_{ij} (bottom) used in Problem 7.

$i \setminus j$	1	2	3	4	5	6	7	8
1		1282.651 0.2	140.3364 0.3	2239.606 0.2	77.37876 0.3	100 0.2	150 0.3	251 0.2
2	–711.399 0.2		–57.649 0.3	–682.468 0.2	–120.713 0.3	–100 0.2	–150 0.2	–200 0.2
3	1196.296 0.3	1030.405 0.3		1097.451 0.3	2214.466 0.2	–300 0.3	–350 0.2	–251 0.3
4	–65.0491 0.2	689.1509 0.2	282.4739 0.3		–86.8052 0.2	1000 0.3	1050 0.3	851 0.3
5	1374.48 0.3	3094.777 0.3	3822.878 0.2	1290.554 0.2		500 0.2	550 0.3	551 0.2
6	1000 0.2	1500 0.2	2000 0.3	–100 0.3	–300 0.2		505 0.2	506 0.2
7	1050 0.3	1550 0.2	2050 0.2	–150 0.3	–350 0.3	–305 0.2		405.1 0.3
8	2051 0.2	2000 0.2	1750 0.3	–151 0.3	–451 0.2	–206 0.2	–305.1 0.3	

Table 9. Pure component physical property data used in Problem 7. Antoine equation coefficients are for the case of P_i^{sat} in mmHg and T in K. Components 1–5 have the same properties as given in Table 6.

	$i = 6$	$i = 7$	$i = 8$
T_{ci} (K)	600	550	451
P_{ci} (kPa)	6000	6050	6100
ω_i	0.2	0.2	0.2
v_i^{L} (cm^3/mol)	80.0	85.0	95.1
A_i	8.0	8.5	7.51
B_i	1700.0	1700.5	1600.51
C_i	200.0	250.0	210.1

Table 10. Results for selected problem sizes and feeds in Problem 7. Feed compositions are given in the text for each problem size.

n	Feed *T* (K) *P* (kPa)	Stationary Points[a,b] $\boldsymbol{x}$; θ; Z	PTPD ($\widetilde{D}$)	CPU time[c] (s)	Result
6	338.15 101.325	(0.148, 0.052, 0.400, 0.100, 0.180, 0.120); 0 (0.0690, 0.0065, 0.5392, 0.1031, 0.2744, 0.0078); 1; 0.9755 (0..0404, 0.0026, 0.0026, 0.0366, 0.8153, 0.1024); 0 (0.0977, 0.0367, 0.6470, 0.0650, 0.0576, 0.0961); 0	0 0.0778 –0.1971 –0.007142	106	Not Stable
6	368.15 101.325	(0.148, 0.052, 0.400, 0.100, 0.180, 0.120); 1; 0.9787 (0.0862, 0.0531, 0.0613, 0.0423, 0.1671, 0.5900); 0	0 0.1931	14.8	Stable (V)
7	428.15 800	(0.148, 0.052, 0.300, 0.100, 0.180, 0.120, 0.100); 1; 0.8846 (0.1092, 0.0709, 0.1369, 0.0599, 0.1480, 0.3959, 0.0793); 0	0 0.1225	295	Stable (V)
7	338.15 101.325	(0.148, 0.052, 0.300, 0.100, 0.180, 0.120, 0.100); 0 (0.0650, 0.0069, 0.4451, 0.0880, 0.1754, 0.0076, 0.2121); 1; 0.9744 (0.1323, 0.0504, 0.4246, 0.0880, 0.1083, 0.1099, 0.0866); 0 (0.0680, 0.0092, 0.0134, 0.0584, 0.5989, 0.1309, 0.1212); 0	0 0.0009064 –0.0006833 –0.04486	535	Not Stable
7	368.15 101.325	(0.148, 0.052, 0.300, 0.100, 0.180, 0.120, 0.100); 1; 0.9793 (0.0763, 0.0438, 0.0338, 0.0389, 0.1873, 0.5971, 0.0227); 0	0 0.1836	1059	Stable (V)
8	418.15 700	(0.148, 0.052, 0.300, 0.100, 0.180, 0.120, 0.060, 0.040); 1; 0.8949 (0..0733, 0.0480, 0.0834, 0.0520, 0.1753, 0.4010, 0.0215, 0.1455); 0	0 –0.1046	1030	Not Stable
8	388.15 600	(0.148, 0.052, 0.300, 0.100, 0.180, 0.120, 0.060, 0.040); 0 (0.1071, 0.0140, 0.3890, 0.1110, 0.2247, 0.0175, 0.1306, 0.0060); 1; 0.8927 (0.1465, 0.0524, 0.3213, 0.0985, 0.1655, 0.1180, 0.0585, 0.0393); 0 (0.0887, 0.0157, 0.0308, 0.0727, 0.5328, 0.1355, 0.0737, 0.0501); 0	0 0.183 –0.00000385 –0.01857	13505	Not Stable
8	418.15 600	(0.148, 0.052, 0.300, 0.100, 0.180, 0.120, 0.060, 0.040); 1; 0.9111 (0.0745, 0.0491, 0.0866, 0.0522, 0.1707, 0.4019, 0.0214, 0.1437); 0	0 0.03337	932	Stable (V)

[a] Mole fractions may not sum precisely to one, due to rounding of computer output during transcription to the table.
[b] A value of the compressibility *Z* is given only for vapor-phase stationary points ($\theta = 1$).
[c] Intel Pentium 4 CPU (3.2 GHz)

List of Figures and Captions

Figure 1. Plot of Gibbs energy surface in Problem 1.

Figure 2. Plot of pseudo tangent plane distance (PTPD) function in Problem 1 for feed composition of $x_{0,1} = 0.6$. This feed is not stable.

Figure 3. Plot of pseudo tangent plane distance (PTPD) function in Problem 3 for vapor-liquid "equilibrium" apparently computed by Uusi-Kyyny et al. [29]. This is not a stable state. See text for discussion.

Figure 4. Phase diagram computed from Uusi-Kyyny et al.'s [29] model in Problem 3, along with their experimental data (■ = vapor; ● = liquid). See text for discussion.

Figure 5 Plot of pseudo tangent plane distance (PTPD) function in Problem 4 for liquid-liquid phase split apparently computed by Kang [30]. This is not a stable state. See text for discussion.

Figure 6. Phase diagram for "hypothetical" system considered in Problem 4. See Figure 7 for enlargement of region around $x_1 \approx 0.8$. See text for discussion.

Figure 7. Enlargement of region around $x_1 \approx 0.8$ in Figure 6. See text for discussion.

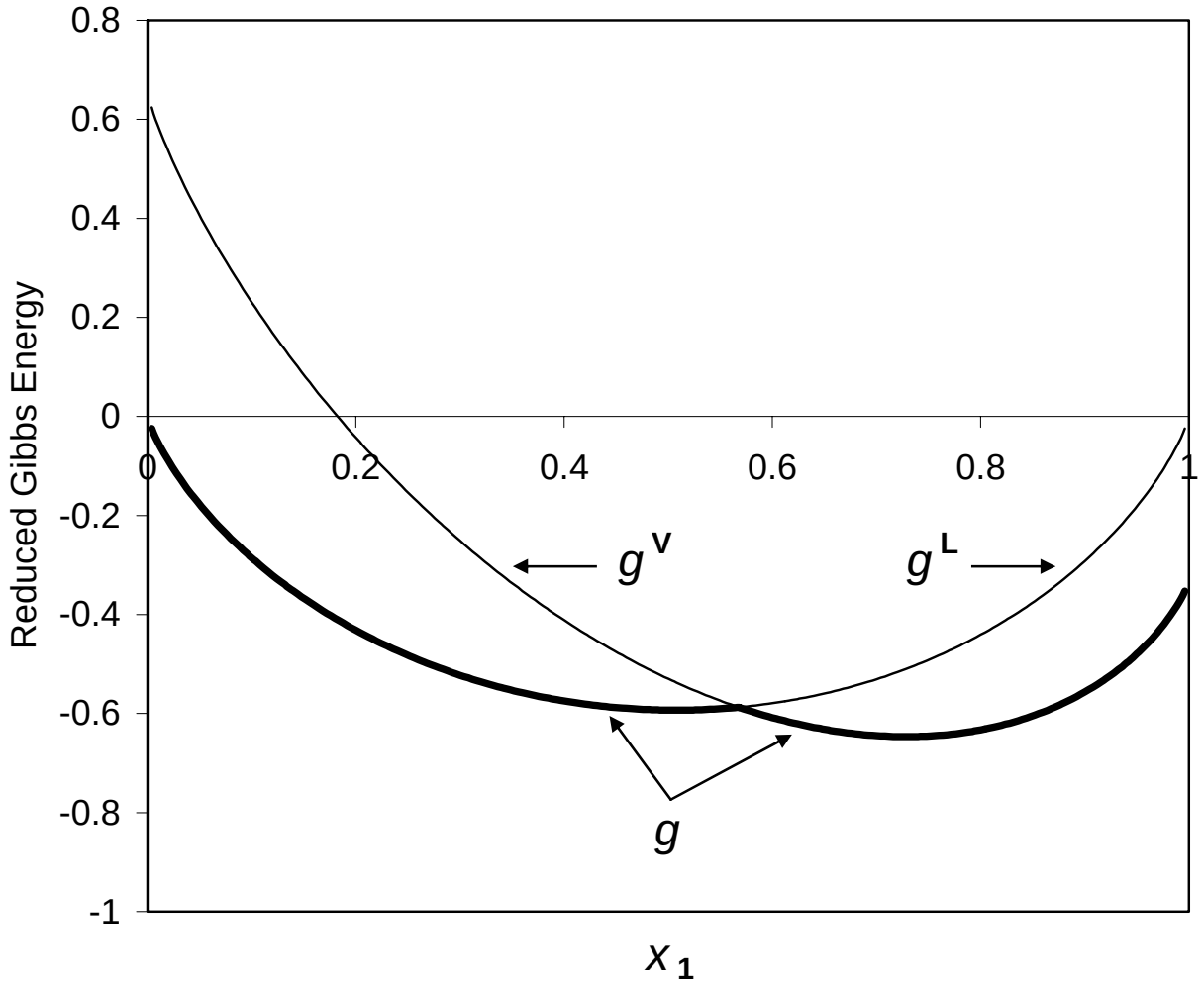

Figure 1. Plot of Gibbs energy surface in Problem 1.

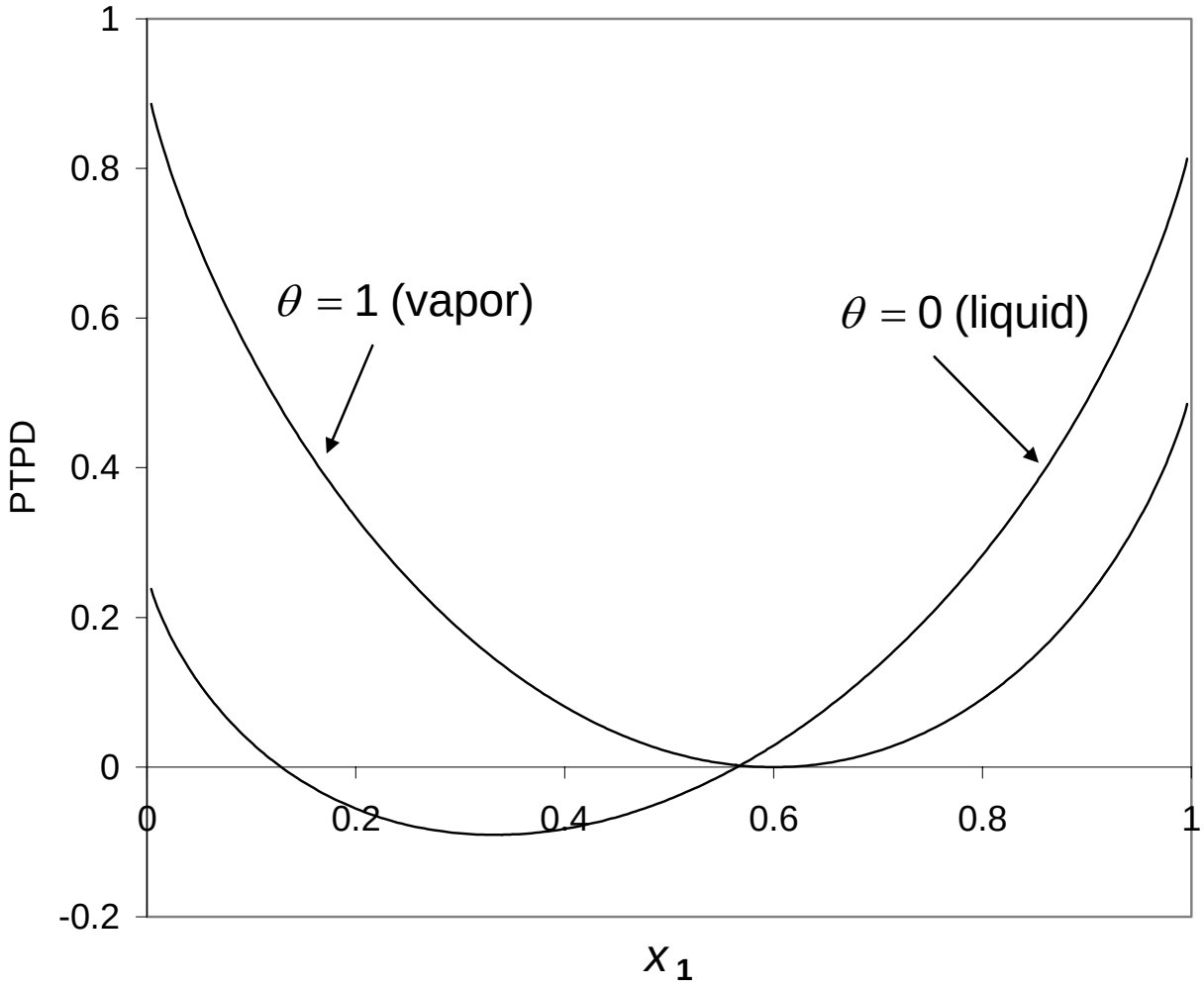

Figure 2. Plot of pseudo tangent plane distance (PTPD) function in Problem 1 for feed composition of $x_{0,1}$ = 0.6. This feed is not stable.

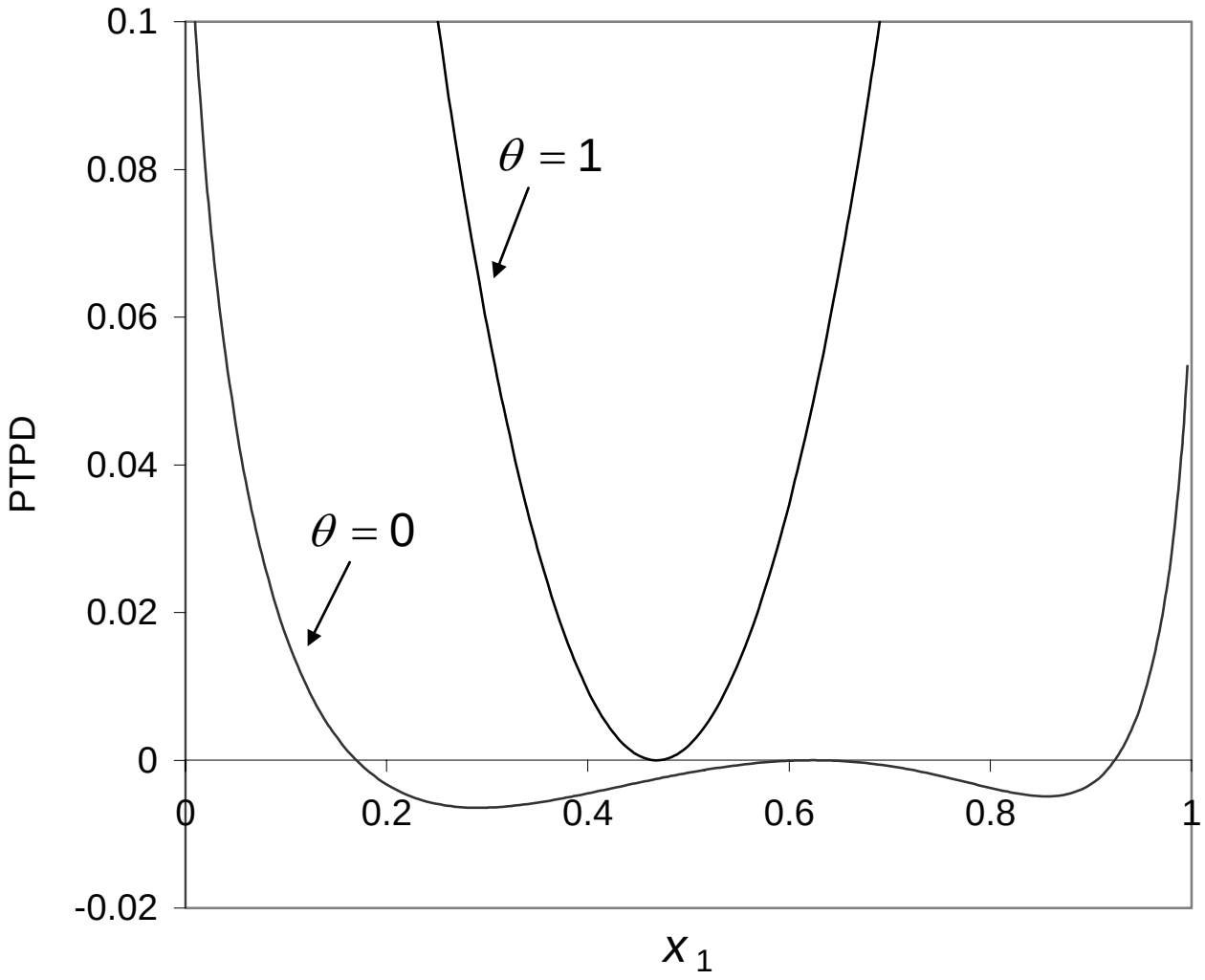

Figure 3. Plot of pseudo tangent plane distance (PTPD) function in Problem 3 for vapor-liquid "equilibrium" apparently computed by Uusi-Kyyny et al. [29]. This is not a stable state. See text for discussion.

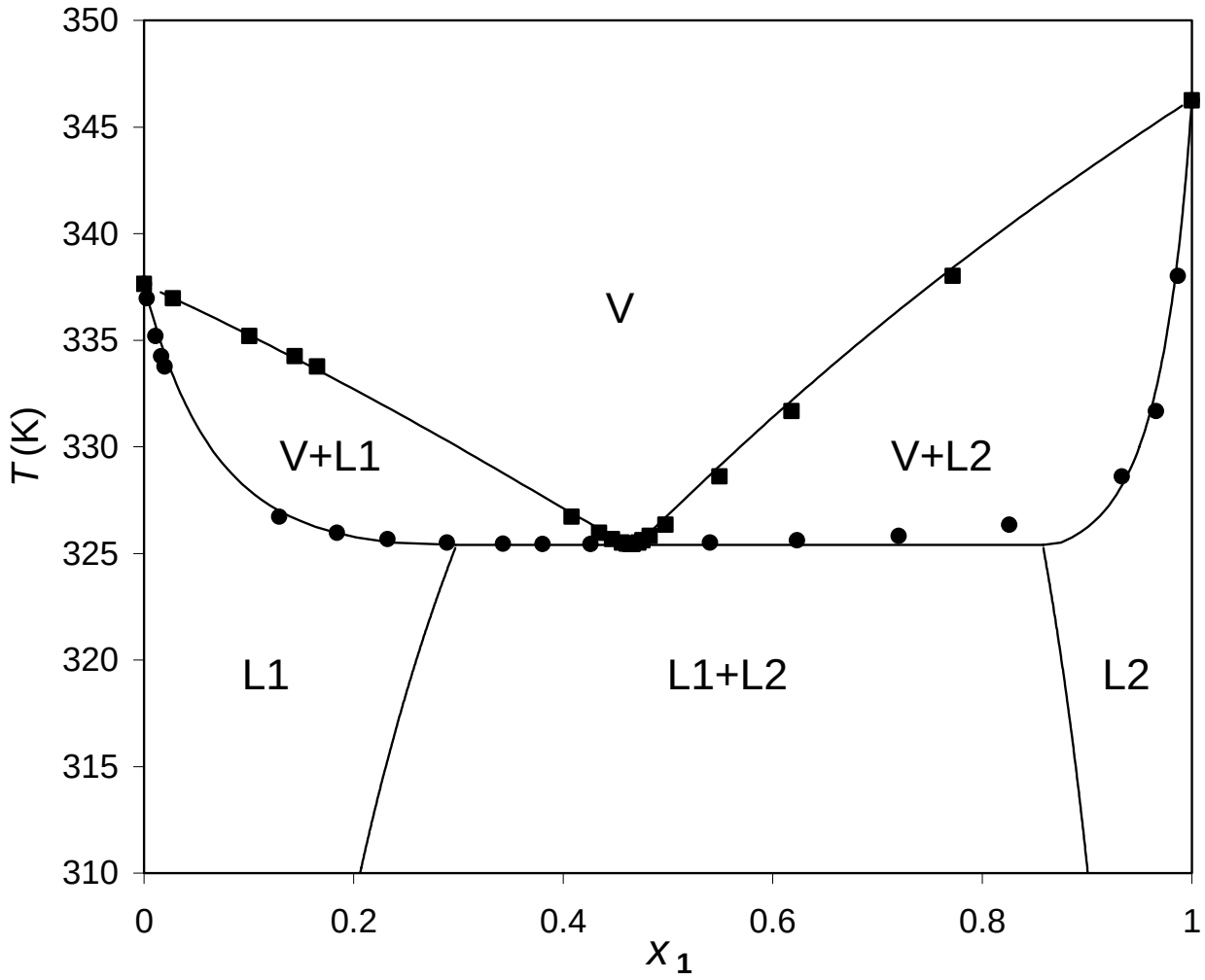

Figure 4. Phase diagram computed from Uusi-Kyyny et al.'s [29] model in Problem 3, along with their experimental data (■ = vapor; ● = liquid). See text for discussion.

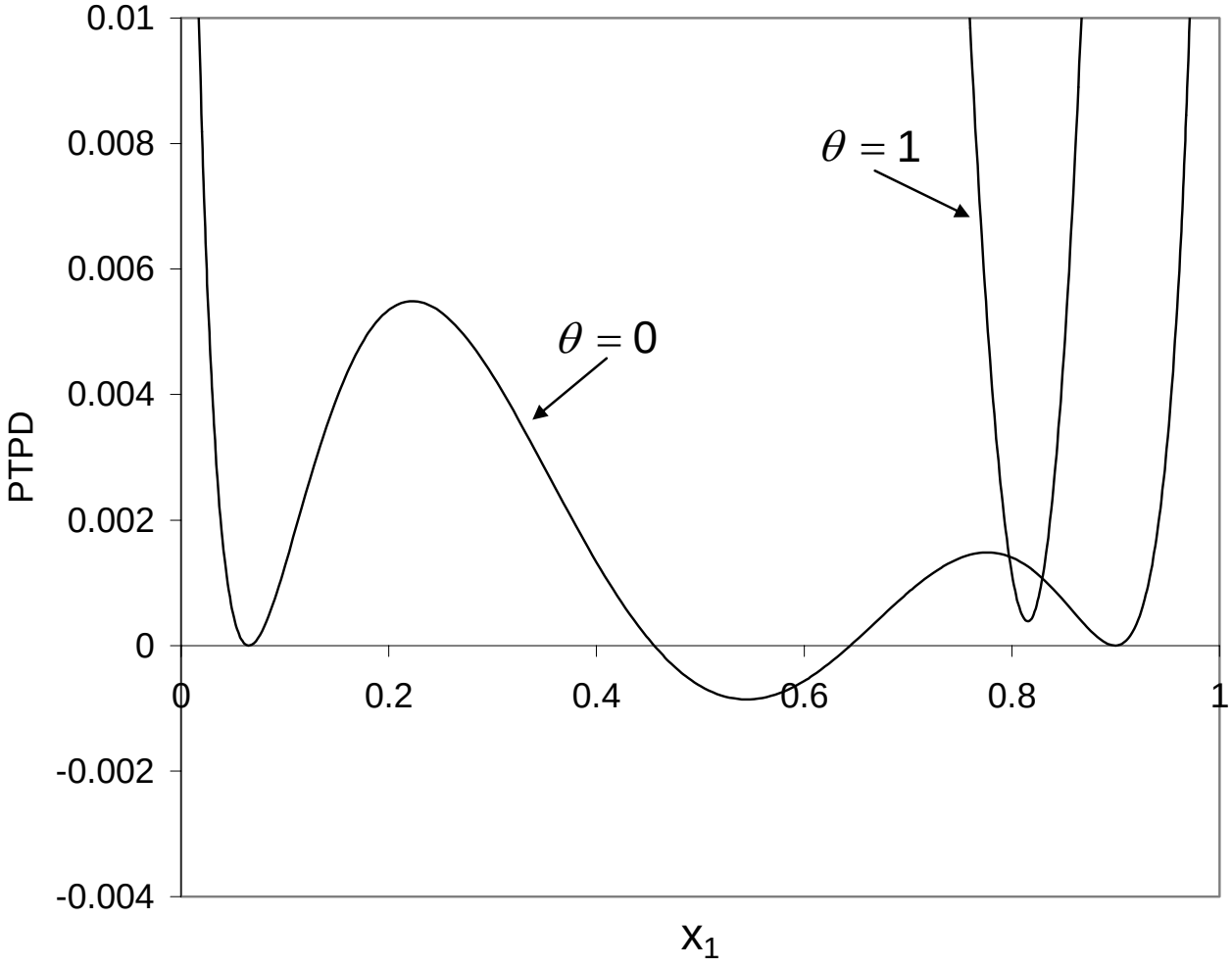

Figure 5 Plot of pseudo tangent plane distance (PTPD) function in Problem 4 for liquid-liquid phase split apparently computed by Kang [30]. This is not a stable state. See text for discussion.

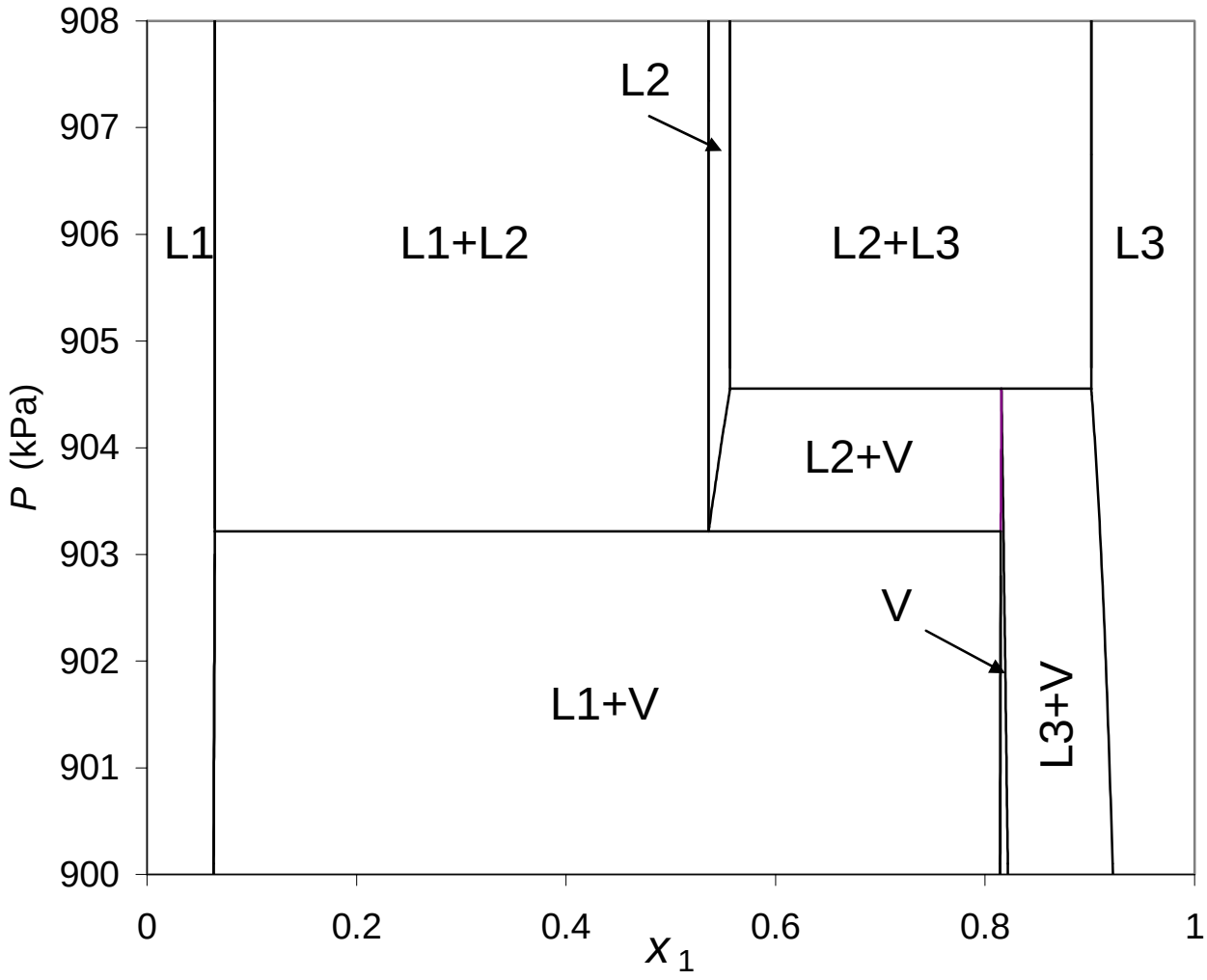

Figure 6. Phase diagram for "hypothetical" system considered in Problem 4. See Figure 7 for enlargement of region around $x_1 \approx 0.8$. See text for discussion.

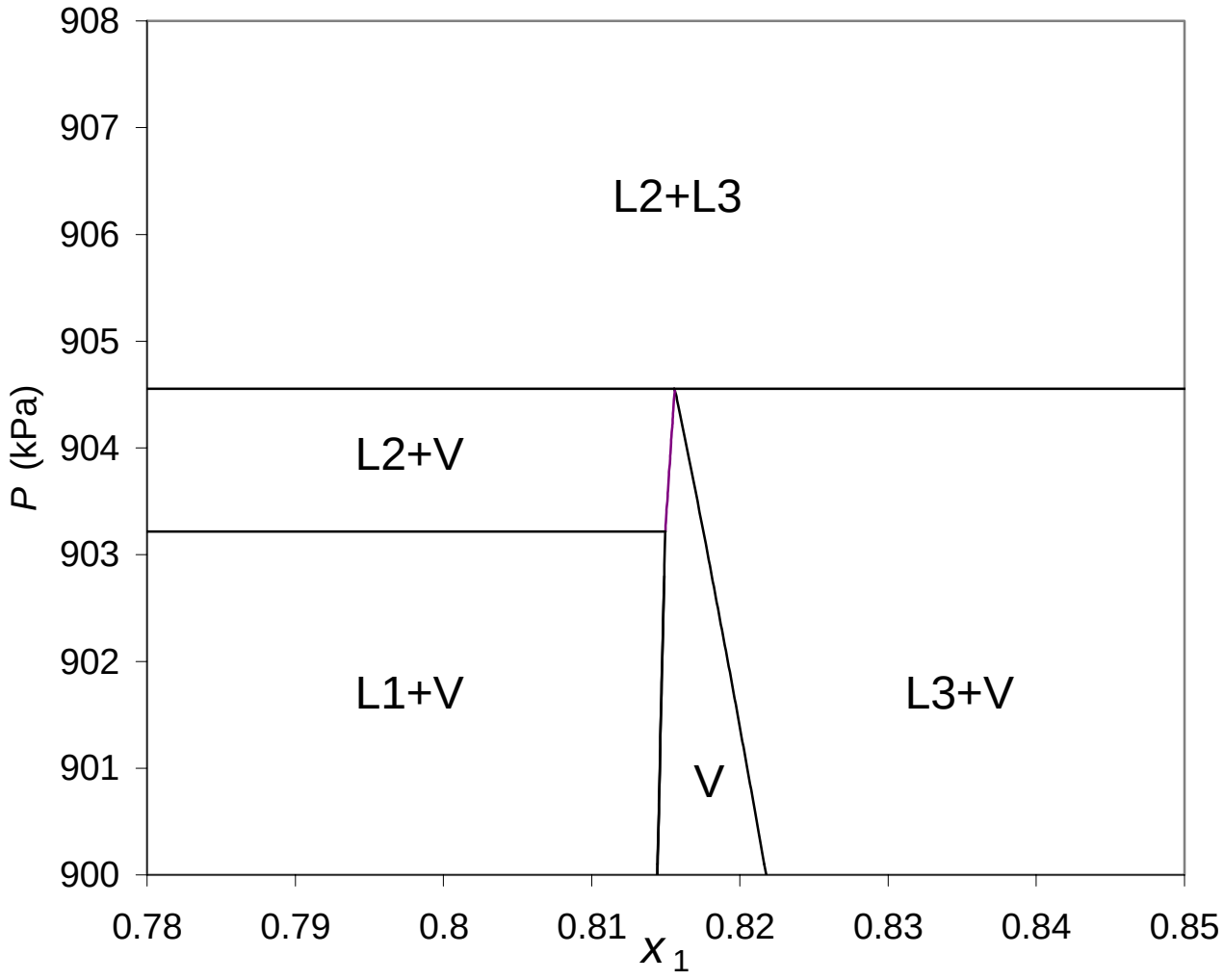

Figure 7. Enlargement of region around $x_1 \approx 0.8$ in Figure 6. See text for discussion.